Biomechanical Correlations Between the Cornea and the Optic Nerve Head

Manqi Pan,[1] Sunny Kwok,[1] Xueliang Pan,[2] and Jun Liu[1,3]

[1]Department of Biomedical Engineering, The Ohio State University, Columbus, Ohio, United States
[2]Department of Biomedical Informatics, The Ohio State University, Columbus, Ohio, United States
[3]Department of Ophthalmology and Visual Sciences, The Ohio State University, Columbus, Ohio, United States

Correspondence: Jun Liu, Department of Biomedical Engineering, The Ohio State University, 4002 Fontana Labs, 140 W. 19th Ave, Columbus, OH 43210, USA;
liu.314@osu.edu.

Received: October 11, 2023
Accepted: May 10, 2024
Published: May 22, 2024

Citation: Pan M, Kwok S, Pan X, Liu J. Biomechanical correlations between the cornea and the optic nerve head. *Invest Ophthalmol Vis Sci.* 2024;65(5):34. https://doi.org/10.1167/iovs.65.5.34

Purpose. A thin cornea is a potent risk factor for glaucoma. The underlying mechanisms remain unexplained. It has been postulated that central corneal thickness (CCT) may be a surrogate for biomechanical parameters of the posterior eye. In this study, we aimed to explore correlations of biomechanical responses between the cornea and the optic nerve head (ONH) and the peripapillary sclera (PPS) to elevated intraocular pressure (IOP), the primary risk factor of glaucoma.

Methods. Inflation tests were performed in nine pairs of human donor globes. One eye of each pair was randomly assigned for cornea or posterior eye inflation. IOP was raised from 5 to 30 millimeters of mercury (mmHg) at 0.5 mmHg steps in the whole globe and the cornea or the ONH/PPS was imaged using a 50 MHz ultrasound probe. Correlation-based ultrasound speckle tracking was used to calculate tissue displacements and strains. Associations of radial, tangential, and shear strains at 30 mmHg between the cornea and the ONH or PPS were evaluated.

Results. Corneal shear strain was significantly correlated with ONH shear strain ($R = 0.857$, $P = 0.003$) and PPS shear strain ($R = 0.724$, $P = 0.028$). CCT was not correlated with any strains in the cornea, ONH, or PPS.

Conclusions. Our results suggested that an eye that experiences a larger shear strain in the cornea would likely experience a larger shear strain in its ONH and PPS at IOP elevations. The strong correlation between the cornea's and the ONH's shear response to IOP provides new insights and suggests a plausible explanation of the cornea's connection to glaucoma risk.

Keywords: ocular biomechanics, ultrasound elastography, cornea, optic nerve head (ONH), mechanical strains

Glaucoma is an optic neuropathy with progressive vision loss. It is the second leading cause of blindness worldwide. Primary risk factors for glaucoma include high intraocular pressure (IOP), older age, black race or Hispanic ethnicity, and thin central corneal thickness (CCT).[1–3] Among these, a thin CCT is considered an independent and potent risk factor for glaucoma development in patients with ocular hypertension, as discovered by the Ocular Hypertension Treatment Study (OHTS)[1] and its follow-up studies.[4,5] CCT has now become an integral part of the clinical workup for diagnosis and treatment planning of glaucoma patients and glaucoma suspects.[6,7]

The reason why CCT is connected to glaucoma risk remains unclear. There are no intuitive explanations because the cornea is not anatomically or physiologically connected to the optic nerve head (ONH), the site of glaucoma damage. Previous studies have evaluated CCT's correlation with sclera thickness, but the results are inconclusive. For the studies performed in donor eyes, CCT's uncertain postmortem change poses a confounding factor as the extent of corneal swelling is uncontrolled, varying with globe recovery time or storage method.[8] Currently there is no established method to obtain in vivo posterior sclera thickness in the human eye. Therefore, studies have attempted to evaluate CCT's correlation with anterior scleral thickness.[9–11] However, sclera thickness varies from anterior to posterior,[12] and previous studies have shown that the anterior and posterior scleral thickness are not correlated in the human eye.[8]

Other studies have evaluated cornea's biomechanical properties and their relationship with glaucoma progression. A lower corneal hysteresis (CH) was found to be a strong predictor of higher glaucoma risk and worse progression.[13–16] The correlation between corneal biomechanics and glaucoma is intriguing, suggesting that biomechanics may be an underlying factor. In this study, we asked the question: is there a biomechanical correlation between the cornea and the tissues in the posterior eye? If such a correlation exists, the cornea's connection with glaucoma might be through the biomechanical similarities between the anterior and the posterior eye.

In this study, we used high-frequency ultrasound elastography[17–19] to measure the tissues' responses to IOP elevation, the primary risk factor of glaucoma, in the intact whole globes with minimal alterations (no fixation or surface

treatment). We have previously validated the elastography technique in terms of its accuracy and sensitivity for measuring ocular tissue deformation.[17,20–22] The 50 MHz linear array ultrasound probe provides an axial resolution of 35 µm and a lateral resolution of 75 µm, and a penetration depth of 1 to 2 mm, enabling high-resolution imaging through the thickness of the cornea, the ONH, and the peripapillary sclera (PPS). More importantly, the analysis of radiofrequency (RF) data achieves a displacement sensitivity of 10s of nanometers.[23,24] An additional advantage of our elastography method is that it outputs all types of mechanical responses to a physiological loading and characterizes tensile, compressive, and shear strains, not limiting to any type of deformation. Using this method, we measured the mechanical responses of the cornea and the ONH/PPS to elevated IOP in paired donor eyes to investigate the association of the responses between the cornea and the tissues in the posterior eye.

Methods

Donor Globes

Nine pairs of donor globes were obtained from the Lion's Eye Bank of West Central Ohio (Dayton, OH, USA). Donor age ranged from 39 to 76 years old (2 male and 7 female donors). Donors with any known ocular diseases, ocular trauma, or ocular surgeries were excluded. Globes with tissue damage during handling (i.e. cornea puncture) were also excluded. The globes were recovered within 18 hours postmortem and experiments were completed within 36 hours postmortem. The superior side of the globe was marked with a tissue ink by Lion's Eye Bank technicians at globe recovery. The corneas remained transparent and did not change in opacity from the time they were received in our laboratory to the completion of the experiments. CCT was first measured by the Lion's Eye Bank technicians at the time of globe recovery using an ultrasound pachymeter (Palmscan AP2000; Micro Medical Devices Inc., Calabasas, CA, USA). The donor globes were stored at 4°C in moist chambers until experimental use.

One eye of each pair was randomly assigned for imaging the cornea's response during IOP increase, and the other was used for imaging the posterior eye including the ONH and the PPS on both sides of the ONH.

For the globes that were assigned for posterior eye inflation testing, extraocular tissue was first removed, and the optic nerve was trimmed to about 1 to 2 mm from the surface of the sclera. The globes were immersed in phosphate buffered saline (PBS) during inflation.

For the globes that were assigned for corneal inflation testing, they were first immersed in and perfused with 4.25% poloxamer 188 (P188) in PBS at 4°C for at least 18 hours to reduce corneal swelling and return the cornea to its physiological hydration following our published protocol.[25] IOP was maintained at 15 millimeters of mercury (mmHg) during the poloxamer treatment. CCT was measured using an ultrasound pachymeter (DGH-550 Pachette 2; DGH Technology, Inc., Exton, PA, USA) before and after the poloxamer treatment. CCT was also estimated from the scanned ultrasound images at the baseline IOP (i.e. 5 mmHg) by fitting two concentric circles to the anterior and posterior boundaries of the cornea. The globes were immersed in the same poloxamer/PBS solution during cornea inflation tests to stabilize corneal thickness.

Inflation Testing With High-Frequency Ultrasound Data Acquisition

During inflation testing, the globes were secured to a custom-built chamber with the imaging side (i.e. cornea or ONH) facing up (Fig. 1A). Two 20 G spinal needles were inserted into the anterior chamber via the limbus, one connected to an infusion pump (Ph.D. Ultra, Harvard Apparatus, Holliston, MA, USA) and the other connected to a pressure sensor (P75, Harvard Apparatus) to monitor and continuously record the IOP. The globes were first preconditioned with 20 cycles from 5 to 30 mmHg at 4 seconds per cycle and left to equilibrate at 5 mmHg for 30 minutes. Previous studies showed[26–28] (consistent with our observation) that tissue response stabilized within the first few cycles and there were minimal preconditioning effects during whole globe inflation within the physiological pressure range. The inflation tests were then performed by increasing IOP from 5 to 30 mmHg with 0.5 mmHg steps (Fig. 1B). The IOP was held constant at each level for 30 seconds before ultrasound scans using a 50 MHz probe (MS700, Vevo2100, FujiFilm VisualSonics, Inc., Toronto, Ontario, Canada). Control of the testing apparatus and data acquisition were implemented using a customized LabView program (National Instruments, Austin, TX, USA). Each inflation test took about 25 minutes to complete for a total of 51 pressure steps. The globes were scanned either along the nasal-temporal (NT) or superior-inferior (SI) direction capturing approximately 9.7 mm in width centered at either the corneal apex or the ONH.

Ultrasound Elastography and Strain Analysis

A correlation-based ultrasound speckle tracking algorithm[17] was used to compute tissue displacements and strains at each step of IOP elevation. Digitized ultrasound RF data were sampled at 1.5 µm × 19 µm (axial × lateral). Regions of interest (ROI) were defined in the reference RF data obtained at the initial IOP. For cornea scans, the ROI was manually defined in the scanned image to include the central 5 mm of the corneal stroma, bound by the anterior and posterior corneal surfaces corresponding to the bright boundaries in the image. For the posterior eye scans, the ROIs for the ONH and the PPS were defined by manual segmentation. We have previously shown an excellent interobserver repeatability (Cronbach Coefficient $\alpha > 0.99$) for strain analysis based on the manual segmentation.[29] Within the cornea ROI, the RF data were divided into kernels, each containing 101 × 41 pixels (axial × lateral), or approximately 150 µm × 780 µm in size, with a 75% overlap to improve spatial resolution of the strain image, following our previous protocols for cornea strain mapping.[30] Within the ONH/PPS ROI, the RF data were divided into kernels, each containing 51 × 31 pixels (axial × lateral), or approximately 75 µm × 570 µm in size, with a 50% overlap, following our previous protocols for ONH/PPS strain mapping.[19,23] The parameters for kernel size and overlap were optimized in our previous studies for the cornea or ONH/PPS speckle tracking, to achieve the best combination of signal-to-noise ratio and strain resolution. PPS thickness was also estimated from the scanned ultrasound images at the initial pressure level by fitting two concentric circles to the anterior and posterior boundaries of the PPS.

The displacement of each kernel was computed by cross-correlation within a search window between RF frames acquired at successive IOP levels. Maximum correlation coef-

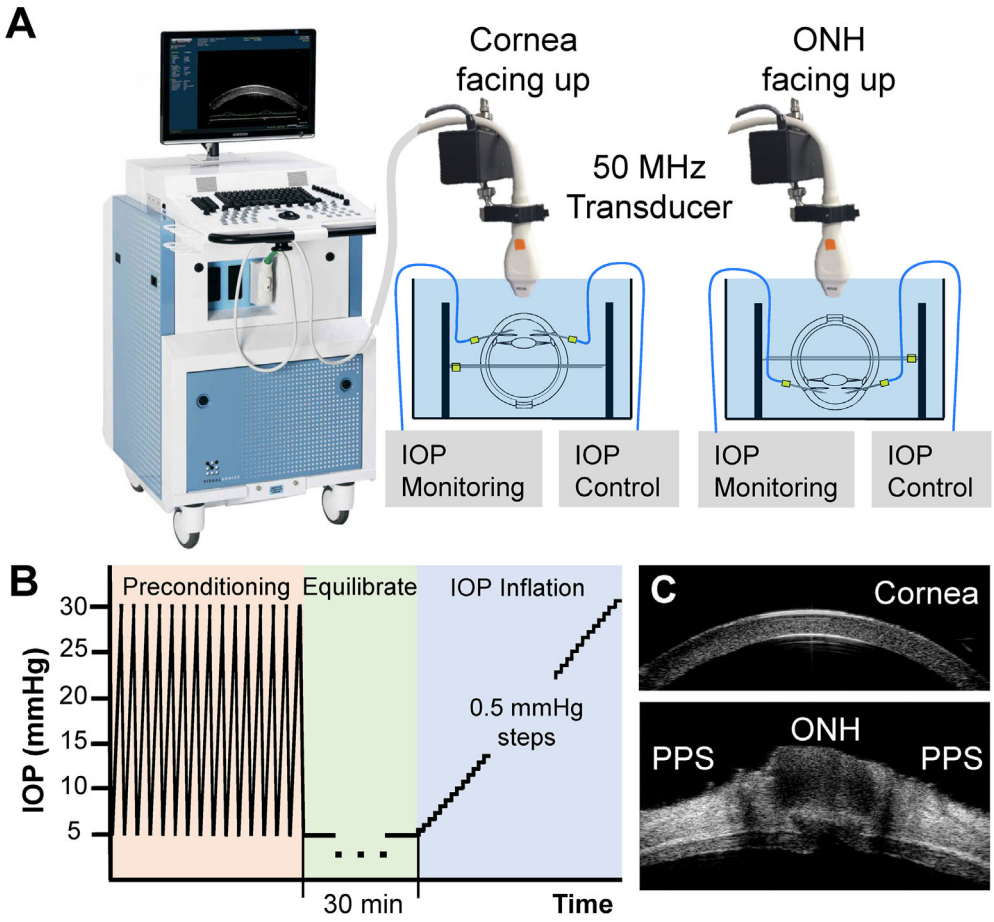

Figure 1. Experimental setup for inflation testing of human donor globes using high-frequency ultrasound elastography. (**A**) One eye of each pair of globes from the same donor was randomly assigned for corneal testing and the other for posterior eye testing. Globes were immersed in poloxamer/PBS (cornea testing) or PBS (posterior eye testing) with IOP control and monitoring. (**B**) Each eye went through the same testing protocol of preconditioning, equilibration, and inflation from 5 to 30 mmHg. (**C**) Representative ultrasound B-mode images of a cornea and a posterior eye.

ficient indicated the best match and the new location of the kernel, and spline interpolation was used to refine the search to achieve subpixel resolution in displacement tracking. The cumulative displacement vectors were calculated with respect to the kernel location at the initial IOP.

Infinitesimal strains (linear approximation of Green-Lagrange strains) were calculated using least squares estimation based on local displacement gradient in a 5 × 5 or 7 × 7 neighborhoods of kernels.[31] Radial, tangential, and shear strains were obtained by coordinate transformation from Cartesian to the polar coordinates based on tissue curvature.[23] Average strains within each region (cornea, ONH, and PPS) at 30 mmHg were used in further analysis. Strain maps were generated to visualize their spatial distribution interpolated to the pixel level.

Statistical Analysis

Mean and standard deviation of radial, tangential, and shear strains at 30 mmHg were summarized for each region (cornea, ONH, and PPS). Associations of radial, tangential, and shear strains between the cornea and ONH or PPS were evaluated using Pearson correlations. Associations between CCT and all types of strains were also explored.

Results

The ultrasound speckles within the ex vivo cornea and ONH/PPS were adequate for successful and reliable speckle tracking, as indicated by high speckle tracking correlation coefficients (>0.95) between consecutive pressure levels in all measured eyes in the current study. Radial, tangential, and shear strains in each region (cornea, ONH, and PPS) increased at higher IOP, as expected (Fig. 2). Representative strain maps at 30 mmHg from one donor are shown in Figure 3.

The overall average radial, tangential, and shear strains at 30 mmHg in the cornea were −1.88 ± 2.08%, 0.50 ± 0.53%, and 5.23 ± 2.38%, respectively. The overall average radial, tangential, and shear strains at 30 mmHg in ONH were −2.96 ± 1.28%, 0.03 ± 0.23%, and 1.67 ± 0.72%, respectively. The overall average radial, tangential, and shear strains at 30 mmHg in PPS were −3.80 ± 0.47%, 0.69 ± 0.57%, and 1.31 ± 0.85%, respectively. Tangential strains were minimal in all regions, whereas radial strains were negative indicating compression. Cornea shear strain was markedly larger than the shear strains in either ONH or PPS (Fig. 4).

Corneal shear strain was significantly correlated with ONH shear strain ($R = 0.857$, $P = 0.003$; Fig. 5A) and PPS

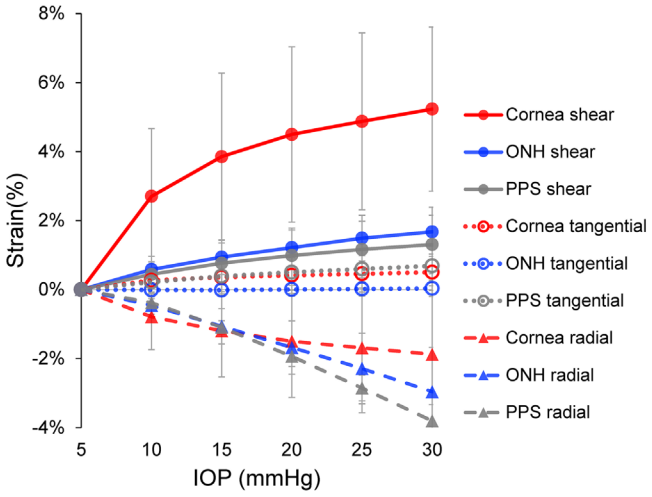

Figure 2. Average radial, tangential, and shear strains in the cornea, the ONH and the PPS in human donor eyes ($N = 9$). All strains increased as IOP increased. Tangential strains were minimal in all three regions.

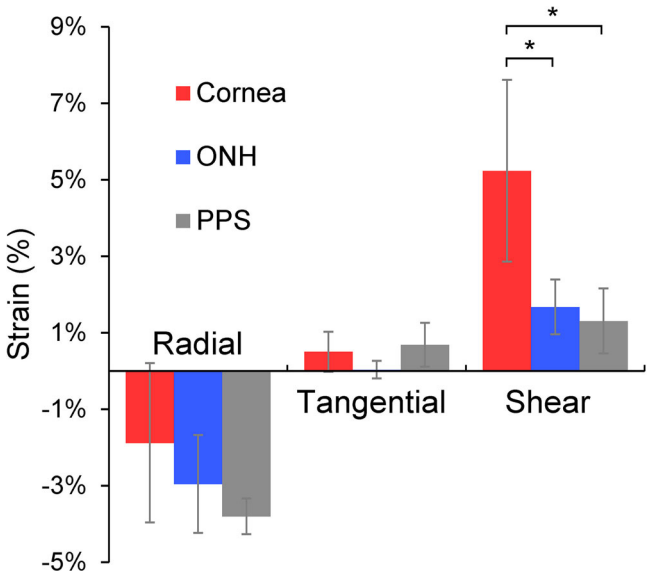

Figure 3. Average radial, tangential, and shear strains in cornea, ONH and PPS at 30 mmHg ($N = 9$). Cornea shear strain was significantly higher than ONH or PPS shear strain (* denotes $P < 0.05$, two-sample *t*-tests).

shear strain ($R = 0.724$, $P = 0.028$; Fig. 5B). Corneal tangential strain was significantly correlated with PPS tangential strain ($R = 0.916$, $P = 0.001$; Fig. 5C). Other types of strains were not significantly correlated between cornea and ONH or PPS. Between ONH and PPS, shear strains were significantly correlated ($R = 0.870$, $P = 0.002$; Fig. 6A). ONH and PPS radial strains were also significantly correlated ($R = 0.744$, $P = 0.022$; Fig. 6B).

The mean CCT measured at various time points was 728.1 ± 73.8 µm at globe recovery, 740.8 ± 76.4 µm before deswelling, 609.2 ± 65.0 µm after deswelling, and 649.2 ± 58.8 µm during inflation tests. Average CCT decreased by 131.6 µm after poloxamer treatment. CCT at globe recovery was significantly correlated with CCT before deswelling ($R = 0.795$, $P = 0.010$). CCT after deswelling was significantly correlated with CCT during inflation ($R = 0.838$, $P = 0.005$). CCT before deswelling was not significantly corre-

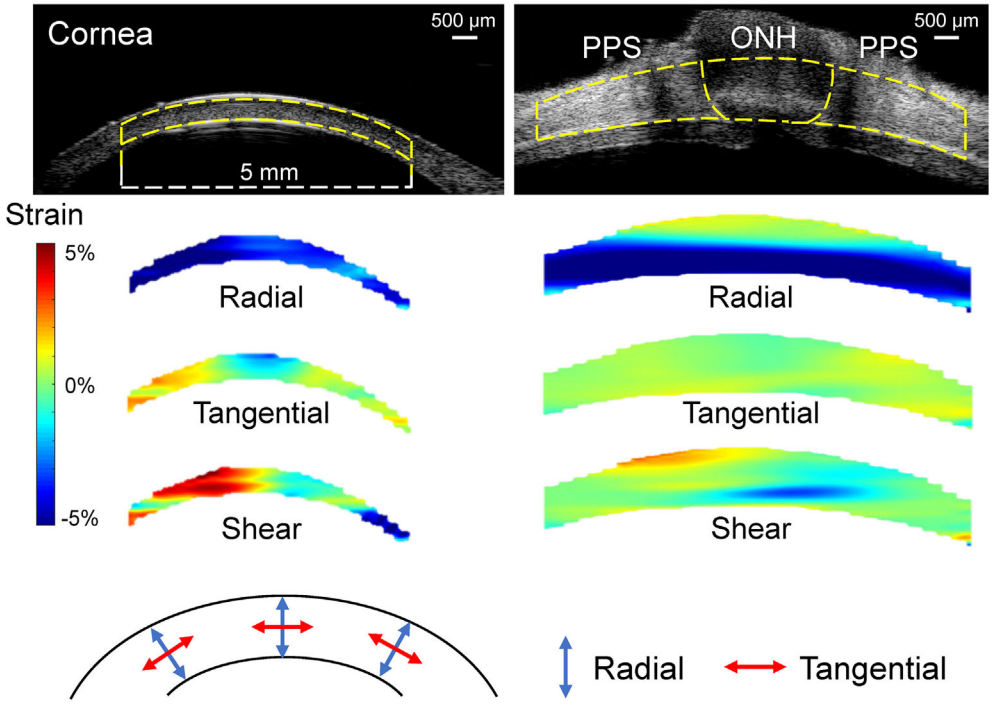

Figure 4. Representative maps of radial, tangential, and shear strains in a cornea and a posterior eye of the same donor at 30 mmHg. As the color bar indicates, *cyan* to *blue* is negative strain (e.g. compression for radial strain), whereas *yellow* to *red* is positive strain (e.g. tensile tangential strain). *Dashed yellow lines* in the ultrasound images delineate the region of interest for strain analysis.

Investigative Ophthalmology & Visual Science

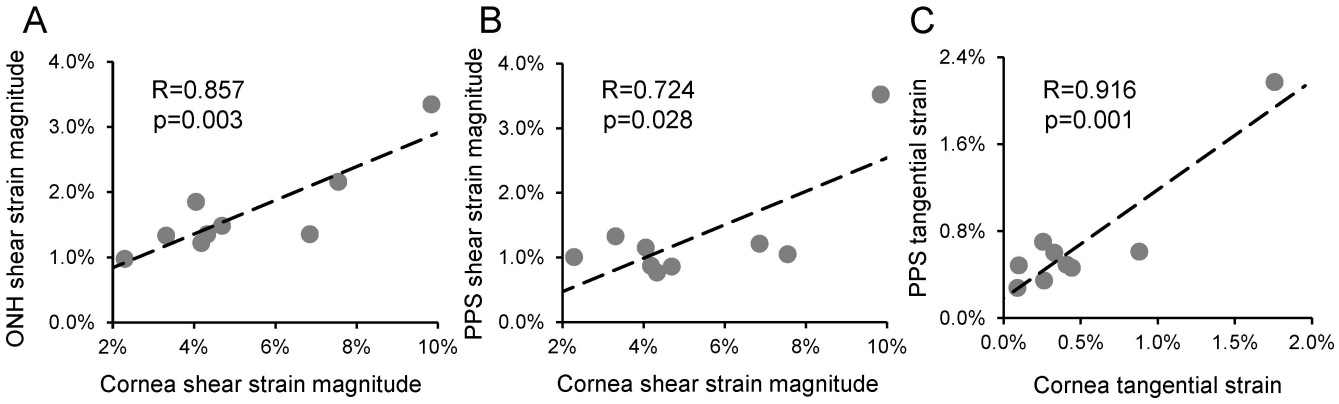

Figure 5. (**A**) Cornea shear strain was significantly correlated with ONH shear strain. (**B**) Cornea shear strain was significantly correlated with PPS shear strain. (**C**) Cornea tangential strain was significantly correlated with PPS tangential strain. One data point of the highest PPS shear and tangential strains may be an outlier that dominated the relationships between PPS and cornea. All strains in this figure were strains at 30 mmHg. Similar correlations were observed at other pressures as well.

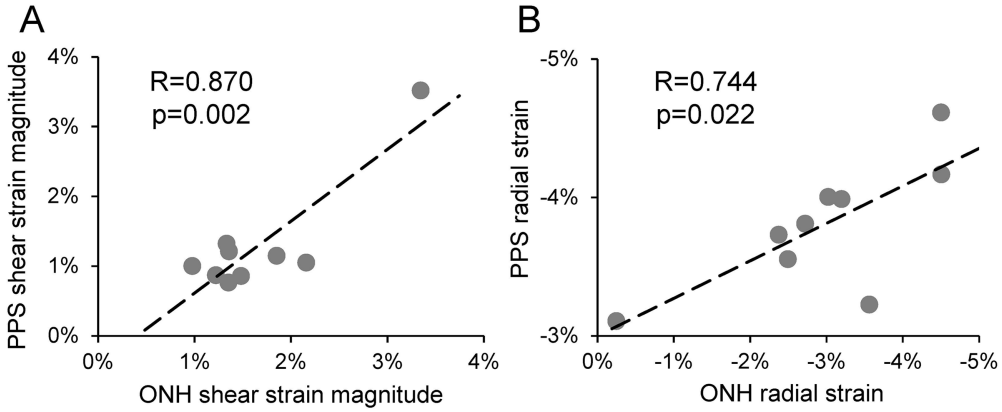

Figure 6. (**A**) ONH shear strain was significantly correlated with PPS shear strain. (**B**) ONH radial strain was significantly correlated with PPS radial strain. All strains in this figure were strains at 30 mmHg. Similar correlations were observed at other pressures as well.

lated with CCT after deswelling ($R = 0.391$, $P = 0.298$). None of these CCT measures was significantly correlated with either the cornea or ONH or PPS strains, partially due to the small sample size. The Pearson correlation between CCT estimated from the cornea's ultrasound scans during inflation and ONH shear strain was 0.213 ($P = 0.582$). None of the CCT measures was correlated with PPS thickness (1043.8 ± 189.2 µm).

Discussion

In this study, we used a high-frequency ultrasound elastography technique to image the mechanical responses of the cornea and the ONH/PPS in paired human donor eyes and explored the biomechanical associations between the anterior and the posterior eye. High-frequency ultrasound imaging has an excellent combination of resolution and penetration depth to characterize all types of mechanical deformation in response to IOP, including the shear strains, which have not been widely reported. The primary finding of this study is that the shear strain in the cornea was strongly correlated with the shear strain in the ONH and PPS of the same donor, suggesting a biomechanical correlation between the anterior and the posterior eye.

Although a low CH has been shown to correlate with more severe glaucoma damage, direct evidence of a relationship between the cornea's biophysical attributes and those of the ONH or PPS is scarce. Previous studies showed that a lower CH in patients with glaucoma was associated with increased deformation of the optic nerve surface during transient IOP elevation; but such correlation was not observed in normal controls.[32] Others have reported a correlation between a lower CH and a thinner scleral thickness in individuals with high myopia[33] and a correlation between a lower corneal deformation amplitude and a larger lamina cribrosa (LC) depth in primary open-angle glaucoma.[34] Our study identified a correlation between the cornea and the ONH's shear response in ostensibly normal donor eyes with no known ocular diseases, indicating a possible presence of a biomechanical relationship between the cornea and the posterior eye likely due to innate structural correspondence.

To some extent, the cornea and the ONH can both be viewed as a mechanical discontinuity in the otherwise continuous scleral shell. Both are mechanically weaker than the sclera and both are surrounded by a circumferential collagen annulus ring[35,36] that prevents large expansion at pressure increase but not outward bending. For a homoge-

neous spherical shell, inflation would create minimal shear. The cornea and the ONH are mechanically distinct from the sclera, which leads to shear deformation during inflation, particularly at the material transition zones. As shown in our previous studies, the shear deformation corresponding to the outward bending concentrates at the conjunction of the ONH and the PPS,[19] a region where glaucomatous damages, such as LC tear and disc hemorrhage,[37,38] often occur. We have also previously reported cornea shear deformation during whole globe inflation based on experimental data and finite element simulations.[39] Others have reported that the cornea's shear modulus is orders of magnitude lower than its young's modulus.[40,41] We observed much larger shear deformation than tensile deformation during inflation, consistent with what would be expected based on the modulus difference although the stresses were also different. The correlation between the cornea's and the ONH/PPS's shear response provides a possible explanation for the connection between the cornea and glaucoma, suggesting that an eye that experiences a larger shear strain in the cornea would also experience a larger shear strain in its ONH/PPS at IOP increase, which could contribute to glaucoma damage. Presumably, a thinner cornea might be less resistant to shear as well; however, we did not observe a correlation between CCT and cornea shear or ONH shear in the current study. One possibility is that residual swelling might still be present in some samples during experimentation, which could confound the CCT data. Future studies are needed to further investigate the potential associations.

Besides the primary finding discussed above, our study also showed that PPS radial and shear strains were correlated with ONH radial and shear strains, respectively. This is a result we repeatedly observed in several studies evaluating ONH and PPS mechanical responses to IOP.[18,19,42] No relationship was identified between CCT and cornea strains in the current study. Interestingly, the association between CCT and CH was also weak to moderate, although both were associated with glaucoma damage.[43] Several studies showed that a low CH was more closely associated with visual field progression than CCT,[13,14,44] suggesting biomechanical properties may play a more important role.

This study has several limitations. First, the preconditioning cycles used a much faster loading rate than the actual inflation tests. We used faster preconditioning cycles to reduce the total experimental time and minimize tissue decay. However, the preconditioning can be affected by loading rate, loading limits, resting periods, and age- or species-related difference in tissue structures.[45] Our preliminary tests in pig and donor eyes showed that tissue displacements generally stabilized after several cycles. This observation was consistent with previous reports of minimal preconditioning effects in pig and human donor eye inflation tests.[26–28] However, given that our preconditioning cycles had a much faster rate than the actual testing, future studies are needed to further optimize the preconditioning protocol to ensure a stabilized response during the actual testing. Second, the sample size of human donor eyes was limited ($N = 9$ pairs, 18 globes), which provided 80% power to detect correlations at $R = 0.8$ and 62% power for $R = 0.7$ at a significance level of 0.05. This sample size does not provide sufficient power to detect weaker correlations that may exist between other types of strains or between CCT and strains. Although the observed strong correlation between the cornea and ONH shear strains was confirmed by both Pearson correlation and Spearman correlation analyses indicating the likelihood of such association, future studies in a larger sample size are needed to verify this result. Another limitation with the small sample size is the potential effect of outliers. One of the tested eyes had a large PPS shear strain and also a large PPS tangential strain. If data from this eye are removed from analysis, correlations between PPS and cornea shear strains (see Fig. 5B) and PPS and cornea tangential strains (see Fig. 5C) would no longer achieve statistical significance. It is noted that the correlation between ONH and cornea shear strains remains significant after removing data from this eye. Interestingly, the PPS was abnormally thin in this eye (approximately 582 µm), suggesting a potential relationship between thin PPS and large PPS shear/tangential strains in response to IOP. Future studies in larger sample sizes are needed to elucidate these relationships. Third, ex vivo tissue may have experienced a certain level of biomechanical alterations as compared to in vivo tissue. Our laboratory has been developing in vivo ultrasound elastography methods to characterize corneal biomechanics[30,46,47] and is pursuing similar techniques for the posterior eye. When these approaches become available, it will offer tools to measure the cornea and posterior eye mechanical responses in vivo to further our understanding of the biomechanical connection between the cornea and the posterior eye and how that impacts an eye's risk for glaucoma. Fourth, we measured the cornea and the ONH/PPS in paired eyes instead of measuring cornea and ONH/PPS in the same eye. Logistically it is difficult for our current imaging setup and protocols to perform inflation tests of both the cornea and the ONH/PPS in the same globe. Dissecting the cornea and ONH/PPS shells are not ideal because dissection could cause damage to the more delicate tissues, such as the retina and the corneal endothelium whose integrity is important for this study. Tissue clamping also introduces unnatural boundary effects. For these reasons, we opted to perform two separate inflation tests in the paired eyes of the same donor. Although there is generally a high degree of interocular symmetry in biometric (e.g. CCT and axial length) and biomechanical parameters (e.g. IOP and corneal displacements) in healthy subjects,[46–50] the potential variance between the left and right eyes could have obscured some correlations and rendered them undetectable in the present study. A comparison between the left and right eyes ONH/PPS shear strains in six pairs of donor eyes is presented in the Supplementary Material to provide data on the potential variance. Our laboratory is currently developing ultrasound-based techniques for in vivo biomechanical characterization of both the cornea and the posterior eye to enable future in vivo studies of their correlations in the same eye.

In conclusion, high-resolution ultrasound elastography was used to explore the correlations between the biomechanical responses of the cornea and those of the ONH and the PPS to IOP elevation, the primary risk factor for glaucoma. We found a strong association between the cornea's shear response and that of the ONH and the PPS, suggesting a biomechanical correlation between the cornea and the tissues in the posterior eye. Future studies are needed to verify this result in vivo, when tools for in vivo characterization of ocular biomechanics become available. Understanding such connection will further elucidate the mechanisms and risk factors underlying glaucoma, providing new insights to improve the diagnosis and treatment of this debilitating disease.

Investigative Ophthalmology & Visual Science

Acknowledgments

Supported by the ARVO Foundation for Eye Research and EyeFind Research Grant and NIHR01EY032621.

Disclosure: **M. Pan**, None; **S. Kwok**, None; **X. Pan**, None; **J. Liu**, None

References

1. Gordon MO, Beiser JA, Brandt JD, et al. The Ocular Hypertension Treatment Study: baseline factors that predict the onset of primary open-angle glaucoma. *Arch Ophthalmol*. 2002;120:714–720; discussion 829-730.
2. Stein JD, Khawaja AP, Weizer JS. Glaucoma in adults-screening, diagnosis, and management: a review. *JAMA*. 2021;325:164–174.
3. Choi J, Kook MS. Systemic and ocular hemodynamic risk factors in glaucoma. *Biomed Res Int*. 2015;2015:141905.
4. Brandt JD, Beiser JA, Gordon MO, Kass MA, Ocular hypertension treatment study group. Central corneal thickness and measured IOP response to topical ocular hypotensive medication in the ocular hypertension treatment study. *Am J Ophthalmol*. 2004;138:717–722.
5. Ocular Hypertension Treatment Study Group, European Glaucoma Prevention Study Group, Gordon MO, et al. Validated prediction model for the development of primary open-angle glaucoma in individuals with ocular hypertension. *Ophthalmology*. 2007;114:10–19.
6. Shih CY, Graff Zivin JS, Trokel SL, Tsai JC. Clinical significance of central corneal thickness in the management of glaucoma. *Arch Ophthalmol*. 2004;122:1270–1275.
7. Patwardhan AA, Khan M, Mollan SP, Haigh P. The importance of central corneal thickness measurements and decision making in general ophthalmology clinics: a masked observational study. *BMC Ophthalmol*. 2008;8:1.
8. Vurgese S, Panda-Jonas S, Jonas JB. Scleral thickness in human eyes. *PLoS One*. 2012;7:e29692.
9. Oliveira C, Tello C, Liebmann J, Ritch R. Central corneal thickness is not related to anterior scleral thickness or axial length. *J Glaucoma*. 2006;15:190–194.
10. Mohamed-Noor J, Bochmann F, Siddiqui MA, et al. Correlation between corneal and scleral thickness in glaucoma. *J Glaucoma*. 2009;18:32–36.
11. Yoo C, Eom YS, Suh YW, Kim YY. Central corneal thickness and anterior scleral thickness in Korean patients with open-angle glaucoma: an anterior segment optical coherence tomography study. *J Glaucoma*. 2011;20:95–99.
12. Norman RE, Flanagan JG, Rausch SM, et al. Dimensions of the human sclera: thickness measurement and regional changes with axial length. *Exp Eye Res*. 2010;90:277–284.
13. Congdon NG, Broman AT, Bandeen-Roche K, Grover D, Quigley HA. Central corneal thickness and corneal hysteresis associated with glaucoma damage. *Am J Ophthalmol*. 2006;141:868–875.
14. Medeiros FA, Meira-Freitas D, Lisboa R, Kuang TM, Zangwill LM, Weinreb RN. Corneal hysteresis as a risk factor for glaucoma progression: a prospective longitudinal study. *Ophthalmology*. 2013;120:1533–1540.
15. Sit AJ, Chen TC, Takusagawa HL, et al. Corneal hysteresis for the diagnosis of glaucoma and assessment of progression risk: a report by the American Academy of Ophthalmology. *Ophthalmology*. 2023;130:433–442.
16. Anand A, De Moraes CG, Teng CC, Tello C, Liebmann JM, Ritch R. Corneal hysteresis and visual field asymmetry in open angle glaucoma. *Invest Ophthalmol Vis Sci*. 2010;51:6514–6518.
17. Tang J, Liu J. Ultrasonic measurement of scleral cross-sectional strains during elevations of intraocular pressure: method validation and initial results in posterior porcine sclera. *J Biomech Eng*. 2012;134:091007.
18. Kwok S, Pan M, Hazen N, Pan X, Liu J. Mechanical deformation of peripapillary retina in response to acute intraocular pressure elevation. *J Biomech Eng*. 2022;144:061001.
19. Ma Y, Pavlatos E, Clayson K, et al. Mechanical deformation of human optic nerve head and peripapillary tissue in response to acute IOP elevation. *Invest Ophthalmol Vis Sci*. 2019;60:913–920.
20. Cruz Perez B, Pavlatos E, Morris HJ, et al. Mapping 3D strains with ultrasound speckle tracking: method validation and initial results in porcine scleral inflation. *Ann Biomed Eng*. 2016;44:2302–2312.
21. Pavlatos E, Perez BC, Morris HJ, et al. Three-dimensional strains in human posterior sclera using ultrasound speckle tracking. *J Biomech Eng*. 2016;138:021015.
22. Ma Y, Pavlatos E, Clayson K, Kwok S, Pan X, Liu J. Three-dimensional inflation response of porcine optic nerve head using high-frequency ultrasound elastography. *J Biomech Eng*. 2020;142:0510131–0510137.
23. Pavlatos E, Ma Y, Clayson K, Pan X, Liu J. Regional deformation of the optic nerve head and peripapillary sclera during IOP elevation. *Invest Ophthalmol Vis Sci*. 2018;59:3779–3788.
24. Pavlatos E, Chen H, Clayson K, Pan X, Liu J. Imaging corneal biomechanical responses to ocular pulse using high-frequency ultrasound. *IEEE Trans Med Imaging*. 2018;37:663–670.
25. Clayson K, Sandwisch T, Ma Y, Pavlatos E, Pan X, Liu J. Corneal hydration control during ex vivo experimentation using poloxamers. *Curr Eye Res*. 2020;45:111–117.
26. Tonge TK, Murienne BJ, Coudrillier B, Alexander S, Rothkopf W, Nguyen TD. Minimal preconditioning effects observed for inflation tests of planar tissues. *J Biomech Eng*. 2013;135:114502.
27. Coudrillier B, Tian J, Alexander S, Myers KM, Quigley HA, Nguyen TD. Biomechanics of the human posterior sclera: age- and glaucoma-related changes measured using inflation testing. *Invest Ophthalmol Vis Sci*. 2012;53:1714–1728.
28. Whitford C, Joda A, Jones S, Bao F, Rama P, Elsheikh A. Ex vivo testing of intact eye globes under inflation conditions to determine regional variation of mechanical stiffness. *Eye Vis (Lond)*. 2016;3:21.
29. Ma Y, Kwok S, Sun J, et al. IOP-induced regional displacements in the optic nerve head and correlation with peripapillary sclera thickness. *Exp Eye Res*. 2020;200:108202.
30. Clayson K, Pavlatos E, Pan X, Sandwisch T, Ma Y, Liu J. Ocular pulse elastography: imaging corneal biomechanical responses to simulated ocular pulse using ultrasound. *Transl Vis Sci Technol*. 2020;9:5.
31. Kallel F, Ophir J. A least-squares strain estimator for elastography. *Ultrason Imaging*. 1997;19:195–208.
32. Wells AP, Garway-Heath DF, Poostchi A, Wong T, Chan KC, Sachdev N. Corneal hysteresis but not corneal thickness correlates with optic nerve surface compliance in glaucoma patients. *Invest Ophthalmol Vis Sci*. 2008;49:3262–3268.
33. Park JH, Choi KR, Kim CY, Kim SS. The height of the posterior staphyloma and corneal hysteresis is associated with the scleral thickness at the staphyloma region in highly myopic normal-tension glaucoma eyes. *Br J Ophthalmol*. 2016;100:1251–1256.
34. Jung Y, Park HL, Park CK. Relationship between corneal deformation amplitude and optic nerve head structure in primary open-angle glaucoma. *Medicine (Baltimore)*. 2019;98:e17223.
35. Newton RH, Meek KM. Circumcorneal annulus of collagen fibrils in the human limbus. *Invest Ophthalmol Vis Sci*. 1998;39:1125–1134.

Investigative Ophthalmology & Visual Science

36. Pijanka JK, Spang MT, Sorensen T, et al. Depth-dependent changes in collagen organization in the human peripapillary sclera. *PLoS One*. 2015;10:e0118648.
37. Sharpe GP, Danthurebandara VM, Vianna JR, et al. Optic disc hemorrhages and laminar disinsertions in glaucoma. *Ophthalmology*. 2016;123:1949–1956.
38. You JY, Park SC, Su D, Teng CC, Liebmann JM, Ritch R. Focal lamina cribrosa defects associated with glaucomatous rim thinning and acquired pits. *JAMA Ophthalmol*. 2013;131:314–320.
39. Kwok S, Hazen N, Clayson K, Pan X, Liu J. Regional variation of corneal stromal deformation measured by high-frequency ultrasound elastography. *Exp Biol Med (Maywood)*. 2021;246:2184–2191.
40. Hatami-Marbini H. Viscoelastic shear properties of the corneal stroma. *J Biomech*. 2014;47:723–728.
41. Petsche SJ, Chernyak D, Martiz J, Levenston ME, Pinsky PM. Depth-dependent transverse shear properties of the human corneal stroma. *Invest Ophthalmol Vis Sci*. 2012;53:873–880.
42. Kwok S, Ma Y, Pan X, Liu J. Three-dimensional ultrasound elastography detects age-related increase in anterior peripapillary sclera and optic nerve head compression during IOP elevation. *Invest Ophthalmol Vis Sci*. 2023;64:16.
43. Zimprich L, Diedrich J, Bleeker A, Schweitzer JA. Corneal hysteresis as a biomarker of glaucoma: current insights. *Clin Ophthalmol*. 2020;14:2255–2264.
44. De Moraes CV, Hill V, Tello C, Liebmann JM, Ritch R. Lower corneal hysteresis is associated with more rapid glaucomatous visual field progression. *J Glaucoma*. 2012;21:209–213.
45. Bianco G, Levy AM, Grytz R, Fazio MA. Effect of different preconditioning protocols on the viscoelastic inflation response of the posterior sclera. *Acta Biomater*. 2021;128:332–345.
46. Kwok S, Clayson K, Hazen N, et al. Heartbeat-induced corneal axial displacement and strain measured by high frequency ultrasound elastography in human volunteers. *Transl Vis Sci Technol*. 2020;9:33.
47. Kwok S, Pan X, Liu W, Hendershot A, Liu J. High-frequency ultrasound detects biomechanical weakening in keratoconus with lower stiffness at higher grade. *PLoS One*. 2022;17:e0271749.
48. Li Y, Bao FJ. Interocular symmetry analysis of bilateral eyes. *J Med Eng Technol*. 2014;38:179–187.
49. Myrowitz EH, Kouzis AC, O'Brien TP. High interocular corneal symmetry in average simulated keratometry, central corneal thickness, and posterior elevation. *Optom Vis Sci*. 2005;82:428–431.
50. Maguire MG. Assessing intereye symmetry and its implications for study design. *Invest Ophthalmol Vis Sci*. 2020;61:27.